

# Quasiparticle energy relaxation times in NbN/CuNi nanostripes from critical velocity measurements

C. Cirillo,<sup>1</sup> V. Pagliarulo,<sup>2</sup> H. Myoren,<sup>3</sup> C. Bonavolontà,<sup>2</sup> L. Parlato,<sup>2</sup> G. P. Pepe,<sup>2</sup> and C. Attanasio<sup>1,\*</sup>

<sup>1</sup>*CNR-SPIN Salerno and Dipartimento di Fisica “E. R. Caianiello”, Università degli Studi di Salerno, Fisciano (Sa) I-84084, Italy*

<sup>2</sup>*CNR-SPIN Napoli and Dipartimento Scienze Fisiche, Università di Napoli Federico II, Facoltà di Ingegneria, I-80125 Napoli, Italy*

<sup>3</sup>*Graduate School of Science and Engineering, Saitama University, 338-8570 Saitama, Japan*

(Received 9 May 2011; published 15 August 2011)

The dynamic instability of the moving vortex lattice at high driving currents in NbN/CuNi-based and NbN nanostripes designed for optical detection has been studied. By applying the model proposed by Larkin and Ovchinnikov [Zh. Eksp. Teor. Fiz. **68**, 1915 (1975)], from the critical velocity  $v^*$  for the occurrence of the instability, it was possible to estimate the values of the quasiparticle relaxation times  $\tau_E$ . The results show that the NbN/CuNi-based devices are characterized by shorter values of  $\tau_E$  compared to that of NbN.

DOI: [10.1103/PhysRevB.84.054536](https://doi.org/10.1103/PhysRevB.84.054536)

PACS number(s): 74.45.+c, 74.78.Fk, 74.40.Gh, 85.25.Oj

## I. INTRODUCTION

In recent years, a large number of works has been devoted to the study of superconducting/ferromagnetic (S/F) hybrids,<sup>1,2</sup> not only regarding fundamental issues such as the consequences of a nonhomogeneous superconducting order parameter in these systems<sup>3–5</sup> and, very recently, the search for the so-called spin-triplet superconductivity,<sup>6–12</sup> but also for the potential application of S/F-based devices such as, for instance, superconducting spin switch,<sup>13–18</sup> superconducting diode,<sup>19</sup> and quantum electronics devices.<sup>20</sup> Lately, the interest in these systems has moved also to nonequilibrium superconductivity. In this field, NbN/CuNi nanostripes showed an increase of the photoresponse amplitude with respect to pure NbN,<sup>21</sup> while Nb/CuNi microbridges presented a reduced slow bolometric contribution compared to the photoresponse of a pure Nb film.<sup>22,23</sup> Moreover, it has been shown that quasiparticle relaxation processes for dirty superconductors,<sup>24</sup> originally calculated as well as experimentally measured with different techniques, are significantly modified in S/F heterostructures. It seems, in fact, that the presence of the ferromagnetic layer reduces the values of the quasiparticle relaxation times  $\tau_E$ .<sup>25–27</sup> This result has been reported for structures consisting of superconducting Nb coupled to F layers characterized by different exchange energy, such as strong Py,<sup>25</sup> as well as weak PdNi (Ref. 26) and CuNi (Ref. 27) ferromagnets. In the last cases, the relaxation processes appear to be modified by the presence of the ferromagnet, as can be inferred from the temperature dependence of  $\tau_E$ .<sup>26,27</sup> However, despite this intense activity, the research in the field of the interplay between superconductivity and ferromagnetism is far from accomplished. In particular, a systematic investigation of both conventional and triplet pairing in S/F structures having nanometric sizes in both thickness and width is lacking. This kind of study would enable the understanding of the evolution of the superconducting state in the one-dimensional (1D) limit. In this direction, pioneering experiments performed on W/Co-based nanowires revealed nonconventional features,<sup>28</sup> while theoretical works suggest that in the 1D regime, the standard singlet S/F proximity effect could become long ranged.<sup>29</sup> For these reasons, the investigation of ultrathin S/F hybrids structured at the nanoscale could represent a new frontier for the research not only in fundamental physics, but also in view of possible applications. In particular, these structures show

appealing properties as ultrafast superconducting radiation detectors due to their unique characteristics in terms of fast response, quantum efficiency, and photon-number resolving capability.<sup>30</sup> Moreover, the achievement of this challenging goal is closely related to the realization of ultrathin S/F hybrids with extremely reduced lateral dimensions, which is a requisite in order to realize highly sensitive detectors. The performances of a potential S/F detector will strongly depend on the choice of the materials, both superconducting and ferromagnetic. Among superconducting materials, NbN is the most promising for application as a photodetector. It is well known, in fact, that NbN guarantees a fast energy relaxation process due to the extremely reduced characteristic electron-phonon (e-ph) coupling time.<sup>31</sup> Moreover, this material is characterized by a short coherence length, which assures that a relatively high superconducting critical temperature  $T_C$  can be obtained even for thicknesses of a few nanometers, so that NbN ultrathin films can have high single-photon sensitivity. The choice of the ferromagnetic materials is also extremely important, since it can strongly influence the critical temperature and the quasiparticle relaxation process of the system. Weak ferromagnetic alloys, such as CuNi,<sup>21–23</sup> have been successfully employed in this research field. In these systems, the magnetic strength can be controlled by the amount of the Ni content in the alloy. Depending on the Ni percentage, the exchange energy  $E_{ex}$  can be tuned in the meV range, leading to a ferromagnetic coherence length,  $\xi_F = \sqrt{\hbar D_F / E_{ex}}$ , of the order of several nanometers,<sup>3,32</sup> therefore comparable to the typical values of the optical penetration depth at the visible light.<sup>22</sup> Finally, compared to Nb/Py structures,<sup>25</sup> PdNi- and CuNi-based bridges present a weaker temperature dependence of the relaxation time,<sup>26,27</sup> which is a feature that could be desirable in the design of a device.

This paper is devoted to the study of the characteristic relaxation rates in NbN/CuNi-based devices estimated in the framework of the model proposed by Larkin and Ovchinnikov (LO),<sup>33</sup> as already reported for different superconducting systems,<sup>34–38</sup> and also for S/F bilayers.<sup>25–27</sup> Superconducting high-velocity vortex lattice instability measurements are presented for a NbN/CuNi system, consisting of six series of three parallel nanostripes that are 300 nm wide, in which the superconducting and the ferromagnetic orders interact via the

proximity effect. The results are compared with those obtained for the same structure made of NbN ultrathin film. This investigation can provide important insight into the relaxation mechanism in S/F hybrids consisting of ultrathin layers patterned at the nanoscale, therefore in limits that have not been explored so far. These results could also provide useful indications for the design of S/F-based photon detectors.

This work is organized as follows. After a brief description of the structure of the samples and of the experimental procedures, results are presented for the preliminary characterization of the samples obtained by measuring critical current density. The central part of the paper deals with the results obtained from the investigation of the vortex lattice instability. Finally, the values of  $\tau_E$  obtained from the analysis of the critical velocity measurements for the two systems are discussed.

## II. SAMPLES AND EXPERIMENTAL METHODS

The devices are realized starting from two plain samples: a single NbN film that is 8 nm thick, and a NbN (8 nm)/CuNi (3 nm) bilayer deposited by dc-magnetron sputtering. The weak ferromagnetic alloy employed in this work has a composition  $\text{CuNi} \equiv \text{Cu}_{0.4}\text{Ni}_{0.6}$ . Details of samples' fabrication are reported elsewhere.<sup>21,39</sup> The sputtered samples have been subsequently patterned by electron beam lithography into a meander-type structure consisting of six serially connected blocks, each containing three parallel wires. The elemental wires have width  $w = 300$  nm and length  $L = 20$   $\mu\text{m}$ . This configuration has been specially designed to improve the performances of nanowire single-photon detectors, since it simultaneously allows a large detection area and fast response, as well as large signal amplitudes.<sup>40</sup> A sketch of the device configuration is reported in the inset of Fig. 1.

Critical temperatures and critical currents  $I_c$  have been resistively measured in a  $^4\text{He}$  cryostat using a standard dc four-probe technique. The  $V(I)$  characteristics have been measured

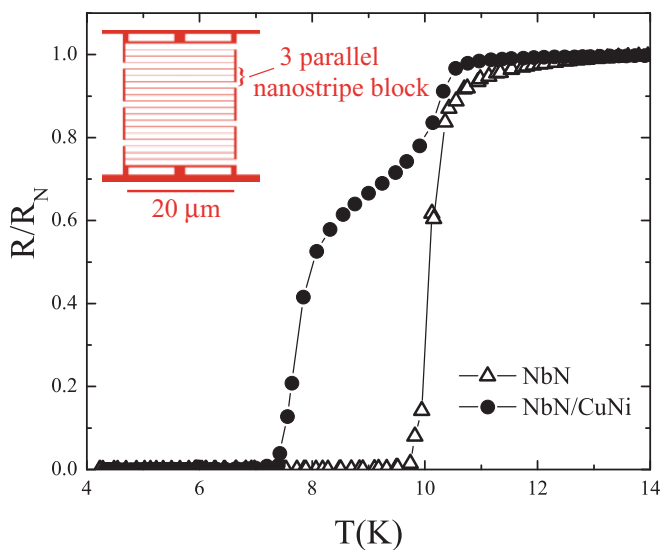


FIG. 1. (Color online) Normalized resistive transition as a function of the temperature for the NbN (open triangles) and the NbN/CuNi (closed circles) devices. Inset: Schematic representation of the device, showing the series of nanostripes' blocks.

both as a function of the temperature and the magnetic field, with the latter being applied always perpendicularly to the samples plane. The temperature stabilization during the measurements was about 1 mK. The values of  $J_c = I_c/wd$  (here  $d$  is the sample thickness) have been extracted using an electric-field criterion of 12 V/m, corresponding to a voltage threshold of 200  $\mu\text{V}$  in the samples, for all the temperatures and fields. In order to avoid possible heating effects, the samples were put into direct contact with the liquid helium and the  $V(I)$  characteristics were measured using a pulsed technique. The current-on time was 12 ms followed by a current-off time of 1 s. Any single voltage value was acquired at the maximum value of the current.

Figure 1 shows the resistive transitions, normalized to the low-temperature normal state resistance  $R_N$ , for both the NbN/CuNi and the NbN devices. Measurements have been performed using a constant bias current  $I_b = 1$   $\mu\text{A}$ . The values of the critical temperature of two samples evaluated at the midpoint of the transitions are  $T_c = 8.04$  K and  $T_c = 10.08$  K, respectively. The transition of the NbN/CuNi structure is clearly broader than the  $R(T)$  of the NbN. This result may reveal the presence of some dishomogeneity of the NbN/CuNi nanostripes at this reduced scale. A detailed analysis of the resistive transitions of both systems is reported in Ref. 21.

## III. CURRENT-VOLTAGE CHARACTERISTICS

### A. Critical current densities

The critical current densities for both structures have been preliminary measured at a zero applied magnetic field. At the lowest reduced temperature,  $t = T/T_c \approx 0.4$ , the values of  $J_c$  for the two systems are  $J_{c,\text{NbN/CuNi}}^{\text{max}} = 1.7 \times 10^{10}$  A/m<sup>2</sup> and  $J_{c,\text{NbN}}^{\text{max}} = 2.2 \times 10^{10}$  A/m<sup>2</sup>. The  $J_c$  values of the NbN/CuNi device are slightly depressed compared to the data reported in Ref. 21. This result could be ascribed to aging effects, with the samples having been stored in air at room temperature for several months after the first measurements. In particular, the degradation in the critical currents values could be a consequence of the relaxation of the disordered CuNi alloy as well as the interdiffusion of the CuNi on the Nb side.<sup>23</sup>

$V(I)$  characteristics have been measured as a function of the magnetic field at  $T = 4.2$  K for the NbN device, and at three different temperatures for the NbN/CuNi, namely,  $T = 4.2, 3.8, 3.5$  K. In Fig. 2, the  $V(I)$  characteristics at  $T = 4.2$  K as a function of the perpendicular applied magnetic field are shown for (a) the NbN structure ( $t = 0.42$ ) and (b) the NbN/CuNi structure ( $t = 0.52$ ). First we comment on the multiple steps present on the resistive branches for both samples, which are due to the switching of the six nanostripe blocks. In the case of the NbN structure, these features are extremely resolved, as is evident from the inset in Fig. 2(a), where the curves are plotted on a semilogarithmic scale. While the analysis of this behavior, already reported for NbN-based meanders,<sup>41</sup> is beyond the scope of this work, the following section discusses the evolution of the first voltage jump. As far as the  $J_c$  is concerned, the behavior of the normalized critical current densities versus the applied magnetic field is shown in Fig. 3, at  $t = 0.42$  and  $t = 0.47$ , for both NbN and NbN/CuNi structures, where the values of  $J_c^{\text{max}}$  are the

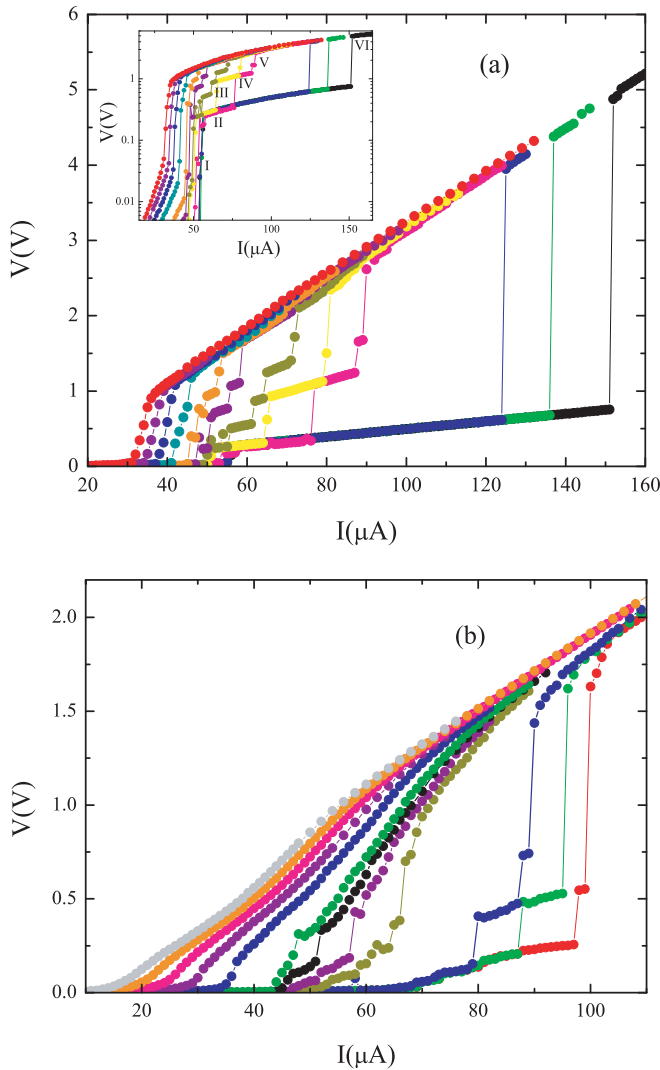


FIG. 2. (Color online)  $V(I)$  characteristics as a function of the magnetic field measured at  $T = 4.2$  K. (a)  $V(I)$  curves for the NbN device measured at a magnetic field of, from right to left, 0, 0.05, 0.10, 0.40, 0.60, 0.80, 1.25, 1.50, 2.00, 2.50, 3.00, and 3.50 T. Inset: The same  $V(I)$  curves on a semilogarithmic scale. Here the steps have been numbered from I to VI for the sake of clarity. (b)  $V(I)$  curves for the NbN/CuNi device measured at a magnetic field of, from right to left, 0, 0.02, 0.05, 0.20, 0.30, 0.40, 0.50, 1.00, 1.50, 2.00, 2.50, and 3.00 T.

ones reported above. The data reveal that both systems present the same field dependence with a small deviation only in an intermediate  $H$  region, probably ascribable to the presence of the ferromagnetic layer. The inset of Fig. 3 shows the temperature dependence of the perpendicular upper critical field,  $H_{c2\perp}(T)$ , of the NbN/CuNi bilayer.

### B. Energy relaxation times

In this section, we will focus on the first abrupt transition to the dissipative state present in the  $V(I)$  characteristics, which have been labeled as I in the inset of Fig. 2(a). This jump is more evident at low values of  $H$ . As the magnetic field is increased, the curves appear in fact more smeared, especially for the NbN/CuNi structure, in which the voltage

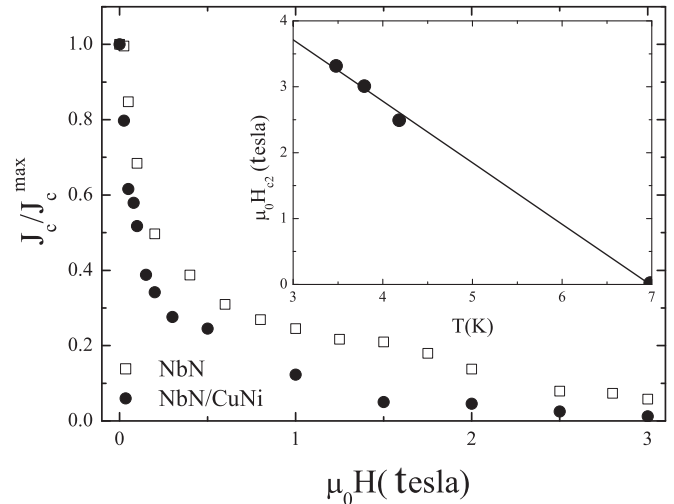


FIG. 3. Normalized critical current density as a function of the magnetic field for the NbN (open squares) and the NbN/CuNi (closed circles) devices. The reduced temperatures are  $t = 0.42$  and  $t = 0.47$ , respectively. Inset: Temperature dependence of the perpendicular upper critical magnetic field,  $H_{c2\perp}(T)$ , of the NbN/CuNi bilayer. The line is a linear fit to the experimental data.

jumps also disappear at relatively moderate fields compared to those of NbN. This abrupt transition can be interpreted in the framework of the model proposed by Larkin and Ovchinnikov (LO)<sup>33</sup> to describe a vortex lattice moving under high applied driving currents. To solve the problem of an inhomogeneous system, such as a type-II superconductor in the mixed state, the Gor'kov equations for the Green's functions have been employed using the Keldysh method. According to the theory of LO, the voltage jumps are a manifestation of the instability of the vortex lattice, which determines the upper limit for the current that the superconductor can sustain. Nonequilibrium effects are a consequence of the variation of the energy distribution inside the vortex core due to the electric field present in the flux-flow state. This energy distribution is, in turn, a direct consequence of the finite inelastic scattering time of the quasiparticles. In the instability regime, the relaxation rate of the quasiparticle energy plays a central role<sup>34</sup> and this, as we said, motivates the interest of this kind of characterization in the case of candidates for optical devices. For a detailed description of the mechanism involved in the instability process and of the limits of validity of the theory, the reader can refer to Ref. 34. Here we stress that at a critical voltage  $V^*$ , the escape of the quasiparticle from the vortex core and the following shrinkage of the latter cause an abrupt transition to the normal state. This critical voltage can be expressed as

$$V^* = \mu_0 v^* H L, \quad (1)$$

where  $v^*$  is the maximum velocity reached by the vortex lattice due to the decrease of the viscous damping,  $H$  is the applied magnetic field, and  $L$  is the distance between the voltage contacts. For the critical velocity, LO obtained the expression

$$v^* = \frac{D^{1/2} [14\zeta(3)]^{1/4} (1-t)^{1/4}}{(\pi\tau_E)^{1/2}}, \quad (2)$$

where  $\zeta(x)$  is the Riemann zeta function,  $D$  is the quasiparticle diffusion coefficient, and  $\tau_E$  is the inelastic relaxation rate of

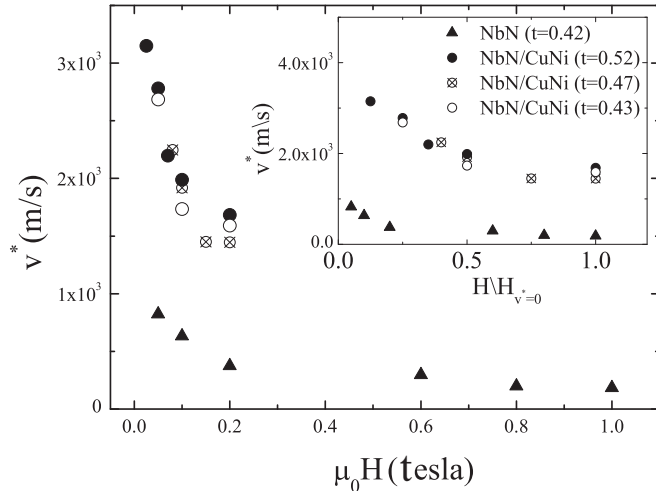


FIG. 4. Critical velocity as a function of the magnetic field for the NbN (solid triangles) and the NbN/CuNi (closed, crossed, and open circles) devices. Inset: The same data are plotted as a function of the reduced field  $H/H_{v^*=0}$ .

the quasiparticles, which therefore can be estimated through critical voltage measurements. Moreover, the temperature dependence of  $\tau_E$  can provide important information regarding the dominant relaxation mechanism. An electron-electron recombination process should provide an exponential behavior, namely,  $\tau_E = \tau_{e-e} \exp(2\Delta(T)/k_B T)$ ,<sup>24</sup> reflecting the exponential temperature dependence of the quasiparticle population. On the other hand, an electron-phonon scattering is governed by the thermal or nonequilibrium phonon population, which reflects in a power-law dependence, that is,  $\tau_E \propto T^{-3}$ .<sup>42</sup> By identifying  $V^*$  as the voltage at which the abrupt transition to the normal state occurs, the values of the critical velocity are directly obtained using Eq. (1). The magnetic field dependencies of  $v^*$  for the NbN device ( $t = 0.42$ ) and for the NbN/CuNi one ( $t = 0.52, 0.47, 0.43$ ) are reported in Fig. 4.

The results confirm the behavior already reported for other S/F systems involving both strong and weak ferromagnets, namely, Nb/Py,<sup>25</sup> Nb/PdNi,<sup>26</sup> and Nb/CuNi.<sup>27</sup> The bilayers in fact present higher critical velocities, which, moreover, disappear at much smaller values of the magnetic field. In the inset, the same behavior is plotted as a function of a reduced field,  $H/H_{v^*=0}$ , where  $H_{v^*=0}$ , once the temperature is fixed, is the maximum field at which the voltage jump is still present. From this graph, the difference in the values of the critical velocity for the two systems can be better appreciated. The saturation value for the NbN meander is in fact  $v^* \approx 180$  m/s, while for the NbN/CuNi it is  $v^* \approx 1500$  m/s. It is interesting to note that even if the model by LO is strictly valid in the case of single superconducting films, this last result is consistent with the dependence reported in Ref. 33 for superconductors with magnetic impurities. In this case, the theory predicts the vortex instability to appear at higher electric fields, that is, at higher critical velocities, due to the fact that the normal excitations are distributed more uniformly over the entire volume of the sample.

By taking into account Eq. (2), it also follows that the values of the relaxation times are substantially different for the two systems. The value of the quasiparticle diffusion

coefficient  $D$  can be estimated from the slope of the  $H_{c2\perp}(T)$  curve.<sup>43</sup> For the NbN structure, we calculated the value of  $D$  from the  $H_{c2\perp}(T)$  curve of the NbN/CuNi bilayer shown in the inset of Fig. 3. This assumption is based on the consideration that in layered S/F systems, the  $H_{c2\perp}(T)$  curves shift in a parallel way compared to the single superconducting film.<sup>44,45</sup> We obtain  $D = (4k_B/\pi e) \times (dH_{c2}/dT|_{T=T_c})^{-1} = 1.2 \times 10^{-4}$  m<sup>2</sup>/s, with  $(dH_{c2}/dT|_{T=T_c}) = -0.93$  T/K. Therefore, the value of the relaxation time estimated for the NbN film at  $t = 0.42$  and at  $\mu_0 H = 1$  tesla ( $H/H_{v^*=0} = 1$ ) is  $\tau_E = 3.5 \times 10^{-9}$  s and at  $\mu_0 H = 0.6$  tesla ( $H/H_{v^*=0} = 0.6$ ) is  $\tau_E = 1.3 \times 10^{-9}$  s. The characteristic times estimated for our NbN structures are about two orders of magnitude shorter than the ones obtained for Nb bridges with the same approach and at the same magnetic field and reduced temperature.<sup>25,26</sup> It is also worth mentioning that even if the values of  $\tau_E$  obtained for the NbN device are higher compared to those estimated from photoresponse experiments, the scaling between the characteristic times of NbN and Nb is consistent with that reported in Ref. 31. The disagreement in the numbers obtained for  $\tau_E$  is probably due to the different techniques applied to investigate the electron relaxation dynamics as a consequence of different excitation energies.<sup>24</sup> In one case, in fact, the nonequilibrium state is photon induced by the formation of a current-assisted hot spot, while in the present study the electron excitations are produced by the electric field at the center of the vortex. From Eq. (2), using the value  $D = 1.2 \times 10^{-4}$  m<sup>2</sup>/s previously calculated, we estimated the value of the relaxation time also for the NbN/CuNi bilayer. The temperature dependence of  $\tau_E$  for the NbN/CuNi meander at  $\mu_0 H = 0.1$  tesla ( $H/H_{v^*=0} = 0.5$ ) is shown in Fig. 5. The first comment is that as a consequence of the results on the critical velocities, the values of the relaxation times for the NbN/CuNi structure are significantly lower than the ones calculated for NbN. In particular, the value of the relaxation time for the NbN/CuNi device at  $t = 0.43$  and at  $\mu_0 H = 0.2$  tesla ( $H/H_{v^*=0} = 1$ ) is  $\tau_E = 4.5 \times 10^{-11}$  s, and at  $\mu_0 H = 0.1$  tesla ( $H/H_{v^*=0} = 0.5$ ) is  $\tau_E = 3.8 \times 10^{-11}$  s.

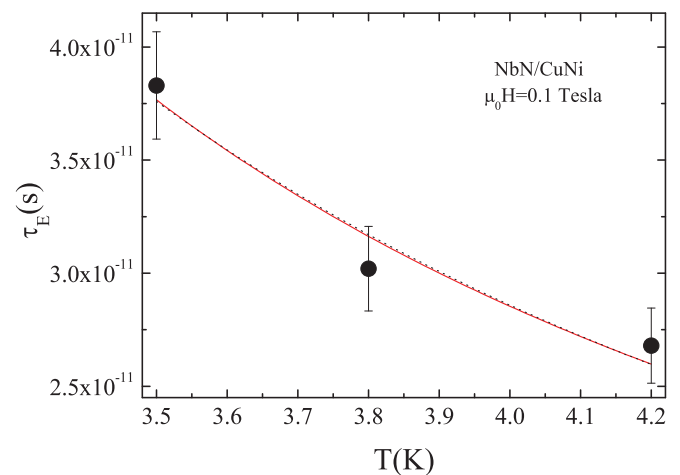


FIG. 5. (Color online) Temperature dependence of the quasiparticle relaxation time for the NbN/CuNi device at  $\mu_0 H = 0.1$  tesla. The black dashed (red solid) line is the power-law (exponential) fit of the experimental data.

Therefore, the relaxation times estimated for our NbN/CuNi devices are about two orders of magnitude shorter than the ones obtained for the NbN nanostructures at the same reduced temperatures  $t$  and magnetic fields  $H/H_{v^*=0}$ . This central result of our investigation seems extremely promising for the design of S/F-based photodetectors. It is well known, in fact, that the performance of the detecting devices, in particular their velocity, crucially depends on the characteristics time  $\tau_{e-ph}$ , which governs electron-phonon interactions.<sup>24</sup> We stress that a faster relaxation process for a superconductor/ferromagnet hybrid compared to its corresponding single S layer is confirmed by an analogous study performed on Nb/Py,<sup>25</sup> Nb/PdNi,<sup>26</sup> and Nb/CuNi<sup>27</sup> bilayers. However, what is interesting to note is that among the analyzed S/F hybrids, the fastest relaxation is obtained for the NbN/CuNi structure. Indeed, for  $t \approx 0.5$  and  $\mu_0 H \approx 0.1$  tesla, the NbN/CuNi system has a value of  $\tau_E$  of about one order of magnitude smaller than Nb/CuNi.<sup>27</sup> Compared to systems with different ferromagnetic layers at the same value of  $t$  and  $\mu_0 H$ , the response of the NbN/CuNi device appears to be two orders of magnitude faster than Nb/PdNi and comparable to NbNb/PdNiPy. Here it is also worth commenting on the fitting procedure performed on the  $\tau_E(T)$  curve, which shows a weak temperature dependence. The solid line in Fig. 5 is the result of the fit according to  $\tau_E = \tau_{e-e} \exp[m\Delta(T)/k_B T]$ , for  $m = 0.5 \pm 0.1$  and  $\tau_{e-e} = 7.7 \times 10^{-12}$  s, where  $\Delta(T) = \Delta(0)(1-t)^{1/2}$  and the gap ratio  $2\Delta(0) = 4.1k_B T_c$  is that of NbN.<sup>46</sup> The value estimated for  $m$  appears to be extremely low due to the comparable values of the critical current density of the NbN/CuNi meander and the NbN. For this reason, the experimental data have also been fitted using a power-law dependence on the temperature for the relaxation time. Following Ref. 42,  $\tau_E$  can be expressed as  $\tau_E \propto T^{-n}$ . The best fit to the experimental data is obtained for  $n = 2.0 \pm 0.5$ , which is not too far from the one expected in the case of a dominant electron-phonon scattering mechanism. The dashed line in Fig. 5 indicates the resulting power-law fit, which can hardly be discerned from the exponential dependence (solid line). Even if more reliable information could be obtained performing the analysis in a wider temperature range, we believe that the results of both fitting procedures suggest that the electron-electron recombination is not responsible for the relaxation mechanism for this system, while it seems reasonable to suppose that the dominant relaxation process is the electron-phonon scattering. A similar temperature dependence of  $\tau_E(T)$  was reported for others S/weak ferromagnetic systems,<sup>26,27</sup> while a stronger temperature dependence was obtained for the NbwPy system.<sup>25</sup> This result was interpreted in Ref. 26 considering that the superconducting correlations are induced deeper inside a weak F layer. On this length, they can interact with a different background, where a different relaxation mechanism can occur. In light of this last result, it is possible to go back to the comparison between the values of  $\tau_E$  for the NbN/CuNi device and the Nb/CuNi and Nb/PdNi systems. Since for all of these structures the electron-phonon scattering is the dominant mechanism, we believe that the significant difference in the relaxation rates is due to the different relaxation properties of the superconducting materials present in the hybrids.

#### IV. CONCLUSIONS

$V(I)$  characteristics have been measured on NbN/CuNi and NbN nanostructures designed for optical detection. The analysis of the experimental data in two different regimes gives information about the behavior of both the critical current density and the vortex lattice instabilities in the two systems. In particular, from the study at high driving currents, it was possible to estimate the values of the quasiparticle relaxation times, which for the NbN/CuNi structure are about two orders of magnitude shorter compared to the values extracted for the corresponding NbN device. Moreover, the smooth temperature dependence of  $\tau_E$  suggests that electron-phonon scattering can be the mechanism responsible for this relaxation, which is in agreement with the results recently reported for other S/weak ferromagnetic systems.<sup>26,27</sup> These results encourage the investigation of the S/F systems in the research for fast nonequilibrium devices. However, the design of a reliable device requires a proper choice of the ferromagnetic materials.

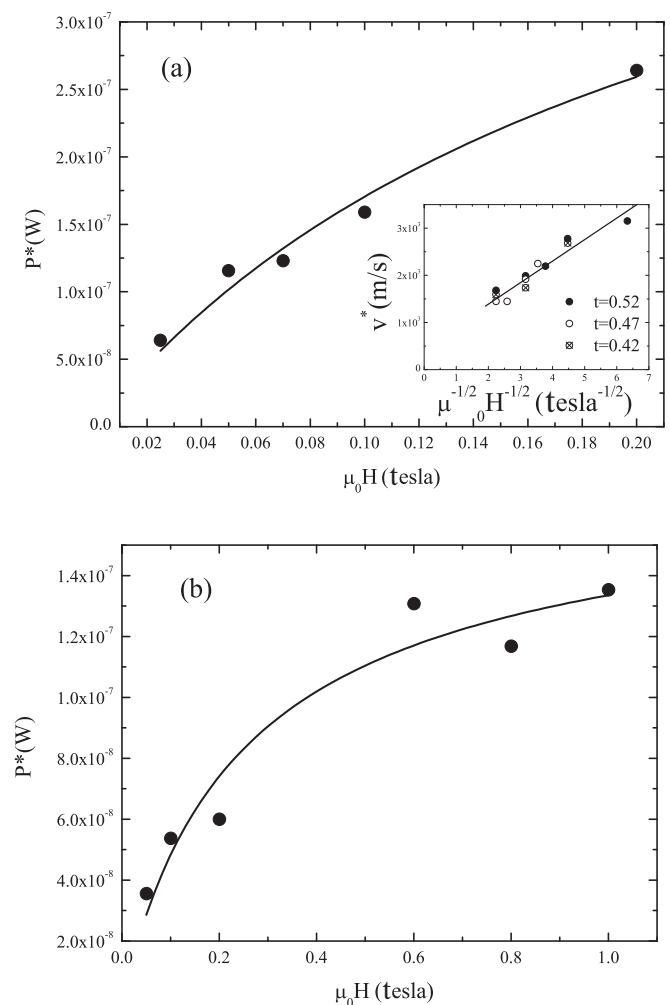


FIG. 6. Dissipated power  $P^*$  as a function of the magnetic field  $\mu_0 H$  at  $T = 4.2$  K for (a) NbN/CuNi and (b) NbN devices. The lines indicate the result of the fitting procedure according to the theory proposed in Ref. 47. Inset: Critical velocity  $v^*$  as a function of  $\mu_0^{-1/2} H^{-1/2}$  for NbN/CuNi at different reduced temperatures. The line is a guide to the eye to show the  $H^{-1/2}$  dependence of  $v^*$ .

In this respect, in order to further reduce the relaxation *times*, it could be interesting to perform the same study on a NbN-based S/F hybrid in which the superconducting layer is coupled with a strong ferromagnetic material. On the other hand, the use of a weak ferromagnet could be more suited to change and tailor the optical properties of the whole system. In particular, an increased electron-phonon interaction could reflect itself in an almost constant value of  $\tau_E$ , which is a feature that could also be important in view of possible applications.

#### APPENDIX: THE PROBLEM OF THERMAL HEATING

As already discussed in Sec. I, special care was paid to minimize any heating effect. However, when plotting the behavior of  $v^*$  as a function of  $H^{-1/2}$  for the NbN/CuNi device, a linear dependence in the low-field regime is revealed. This result, reported in the inset of Fig. 6(a), can in principle

be ascribed to Joule heating.<sup>47</sup> For this reason, the field dependence of the dissipated power  $P^* = I^*V^*$  at the voltage jumps has been analyzed. From a theoretical fit of  $P^*$  as a function of  $\mu_0H$ , the magnetic field at which thermal effects start to influence the flux-flow instability  $H_T$  can be estimated.<sup>47</sup> In Fig. 6, the dissipated power  $P^*$  as a function of the magnetic field is reported for both the (a) NbN/CuNi and (b) NbN devices at  $T = 4.2$  K. The line is a fit to the experimental data using the expression  $P = P_0(1 - a)$ , where  $a = [1 + b + (b^2 + 8b + 4)^{1/2}]$  and  $b = H/H_T$ .<sup>47</sup> From the fitting procedure, we obtain  $\mu_0H_T = 0.37$  T for NbN and  $\mu_0H_T = 0.35$  T for NbN/CuNi. While in the case of NbN the agreement with the theory is rather poor, suggesting that the quasiparticle heating is not dominant in determining the magnetic field dependence of  $v^*$ , in the case of NbN/CuNi,  $\mu_0H_T$  is considerably higher than the field at which our  $\tau_E(T)$  analysis has been performed.

\*Corresponding author: attanasio@sa.infn.it

<sup>1</sup>A. I. Buzdin, *Rev. Mod. Phys.* **77**, 935 (2005).

<sup>2</sup>F. S. Bergeret, A. F. Volkov, and K. B. Efetov, *Rev. Mod. Phys.* **77**, 1321 (2005).

<sup>3</sup>V. V. Ryazanov, V. A. Oboznov, A. Yu. Rusanov, A. V. Veretennikov, A. A. Golubov, and J. Aarts, *Phys. Rev. Lett.* **86**, 2427 (2001).

<sup>4</sup>T. Kontos, M. Aprili, J. Lesueur, and X. Grison, *Phys. Rev. Lett.* **86**, 304 (2001).

<sup>5</sup>V. Zdravkov, A. Sidorenko, G. Obermeier, S. Gsell, M. Schreck, C. Müller, S. Horn, R. Tidecks, and L. R. Tagirov, *Phys. Rev. Lett.* **97**, 057004 (2006).

<sup>6</sup>I. Sosnin, H. Cho, V. T. Petrashov, and A. F. Volkov, *Phys. Rev. Lett.* **96**, 157002 (2006).

<sup>7</sup>R. S. Keizer, S. T. B. Goennenwein, T. M. Klapwijk, G. Miao, G. Xiao, and A. Gupta, *Nature (London)* **439**, 825 (2006).

<sup>8</sup>D. Sprungmann, K. Westerholt, H. Zabel, M. Weides, and H. Kohlstedt, *Phys. Rev. B* **82**, 060505(R) (2010).

<sup>9</sup>M. S. Anwar, F. Czeschka, M. Hesselberth, M. Porcu, and J. Aarts, *Phys. Rev. B* **82**, 100501(R) (2010).

<sup>10</sup>J. W. A. Robinson, G. B. Halász, A. I. Buzdin, and M. G. Blamire, *Phys. Rev. Lett.* **104**, 207001 (2010).

<sup>11</sup>J. Zhu, I. N. Krivorotov, K. Halterman, and O. T. Valls, *Phys. Rev. Lett.* **105**, 207002 (2010).

<sup>12</sup>T. S. Khaire, M. A. Khasawneh, W. P. Pratt Jr., and N. O. Birge, *Phys. Rev. Lett.* **104**, 137002 (2010).

<sup>13</sup>J. Y. Gu, C.-Y. You, J. S. Jiang, J. Pearson, Ya. B. Bazaliy, and S. D. Bader, *Phys. Rev. Lett.* **89**, 267001 (2002).

<sup>14</sup>A. Potenza and C. H. Marrows, *Phys. Rev. B* **71**, 180503(R) (2005).

<sup>15</sup>A. Yu. Rusanov, S. Habraken, and J. Aarts, *Phys. Rev. B* **73**, 060505(R) (2006).

<sup>16</sup>I. C. Moraru, W. P. Pratt Jr., and N. O. Birge, *Phys. Rev. B* **74**, 220507(R) (2006).

<sup>17</sup>G. Nowak, H. Zabel, K. Westerholt, I. Garifullin, M. Marcellini, A. Liebig, and B. H. Jörvarsson, *Phys. Rev. B* **78**, 134520 (2008).

<sup>18</sup>J. Zhu, X. Cheng, C. Boone, and I. N. Krivorotov, *Phys. Rev. Lett.* **103**, 027004 (2009).

<sup>19</sup>G. Carapella, V. Granata, F. Russo, and G. Costabile, *Appl. Phys. Lett.* **94**, 242504 (2009).

<sup>20</sup>A. K. Feofanov, V. A. Oboznov, V. V. Bol'ginov, J. Lisenfeld, S. Poletto, V. V. Ryazanov, A. N. Rossolenko, M. Khabipov, D. Balashov, A. B. Zorin, P. N. Dmitriev, V. P. Koshelets, and A. V. Ustinov, *Nature Phys.* **6**, 593 (2010).

<sup>21</sup>N. Marrocco, G. P. Pepe, A. Capretti, L. Parlato, V. Pagliarulo, G. Peluso, A. Barone, R. Cristiano, M. Ejrnaes, A. Casaburi, N. Kashiwazaki, T. Taino, H. Myoren, and R. Sobolewski, *Appl. Phys. Lett.* **97**, 092504 (2010).

<sup>22</sup>D. Pan, G. P. Pepe, V. Pagliarulo, C. De Lisio, L. Parlato, M. Khafizov, I. Komissarov, and R. Sobolewski, *Phys. Rev. B* **78**, 174503 (2008).

<sup>23</sup>T. Taneda, G. P. Pepe, L. Parlato, A. A. Golubov, and R. Sobolewski, *Phys. Rev. B* **75**, 174507 (2007).

<sup>24</sup>S. B. Kaplan, C. C. Chi, D. N. Langenberg, J. J. Chang, S. Jafarey, and D. Scalapino, *Phys. Rev. B* **14**, 4854 (1976), and references therein.

<sup>25</sup>A. Angrisani Armenio, C. Bell, J. Aarts, and C. Attanasio, *Phys. Rev. B* **76**, 054502 (2007).

<sup>26</sup>C. Cirillo, E. A. Ilyina, and C. Attanasio, *Supercond. Sci. Technol.* **24**, 024017 (2011).

<sup>27</sup>E. A. Ilyina, C. Cirillo, and C. Attanasio, *Eur. Phys. J. B*, doi:10.1140/epjb/e2011-20476-3.

<sup>28</sup>J. Wang, M. Singh, M. Tian, N. Kumar, B. Liu, C. Shi, J. K. Jain, N. Samarth, T. E. Mallouk, and M. H. W. Chan, *Nature Phys.* **6**, 389 (2010).

<sup>29</sup>F. Korschelle, J. Cayssol, and A. Buzdin, *Phys. Rev. B* **82**, 180509(R) (2010).

<sup>30</sup>M. Ejrnaes, R. Cristiano, O. Quaranta, S. Pagano, A. Gaggero, F. Mattioli, R. Leoni, B. Voronov, and G. Gol'tsman, *Appl. Phys. Lett.* **91**, 262509 (2007).

<sup>31</sup>L. Parlato, R. Latempa, G. Peluso, G. P. Pepe, R. Cristiano, and R. Sobolewski, *Supercond. Sci. Technol.* **18**, 1244 (2005).

<sup>32</sup>C. Cirillo, C. Bell, G. Iannone, S. L. Prischepa, J. Aarts, and C. Attanasio, *Phys. Rev. B* **80**, 094510 (2009).

<sup>33</sup>A. I. Larkin and Yu. N. Ovchinnikov, *Zh. Eksp. Teor. Fiz.* **68**, 1915 (1975); *Sov. Phys. JETP* **41**, 960 (1976).

- <sup>34</sup>W. Klein, R. P. Huebener, S. Gauss, and J. Parisi, *J. Low Temp. Phys.* **61**, 413 (1985).
- <sup>35</sup>S. G. Doettinger, S. Kittelberger, R. P. Huebener, and C. C. Tsuei, *Phys. Rev. B* **56**, 14157 (1997).
- <sup>36</sup>Z. L. Xiao, P. Voss-deHaan, G. Jakob, Th. Kluge, P. Haibach, H. Adrian, and E. Y. Andrei, *Phys. Rev. B* **59**, 1481 (1999).
- <sup>37</sup>C. Peroz and C. Villard, *Phys. Rev. B* **72**, 014515 (2005).
- <sup>38</sup>G. Grimaldi, A. Leo, D. Zola, A. Nigro, S. Pace, F. Laviano, and E. Mezzetti, *Phys. Rev. B* **82**, 024512 (2010).
- <sup>39</sup>H. Myoren, Y. Mada, Y. Matsui, T. Taino, and S. Takada, *J. Phys.* **97**, 012329 (2008).
- <sup>40</sup>M. Ejrnaes, A. Casaburi, O. Quaranta, S. Marchetti, A. Gaggero, F. Mattioli, R. Leoni, S. Pagano, and R. Cristiano, *Supercond. Sci. Technol.* **22**, 055006 (2009).
- <sup>41</sup>F. Mattioli, R. Leoni, A. Gaggero, M. G. Castellano, P. Carelli, F. Marsili, and A. Fiore, *J. Appl. Phys.* **101**, 054302 (2007).
- <sup>42</sup>A. I. Larkin and Yu. N. Ovchinnikov, *Zh. Eksp. Teor. Fiz.* **73**, 299 (1977); *Sov. Phys. JETP* **46**, 155 (1977).
- <sup>43</sup>J. Guimpel, M. E. de la Cruz, F. de la Cruz, H. J. Fink, O. Laborde, and J. C. Villegier, *J. Low Temp. Phys.* **63**, 151 (1986).
- <sup>44</sup>C. Cirillo, S. L. Prischepa, M. Salvato, and C. Attanasio, *Eur. Phys. J. B* **38**, 59 (2004).
- <sup>45</sup>P. Koorevaar, Y. Suzuki, R. Coehoorn, and J. Aarts, *Phys. Rev. B* **49**, 441 (1994).
- <sup>46</sup>M. S. Pambianchi, S. M. Anlage, E. S. Hellman, E. H. Hartford Jr., M. Bruns, and S. Y. Lee, *Appl. Phys. Lett.* **64**, 244 (1994).
- <sup>47</sup>A. I. Bezuglyj and V. A. Shklovskij, *Physica C* **202**, 234 (1992).